Clay mineralogy and diagenesis of the Recent-Pleistocene volcanogenic sedimentary sequence of the Mexican Basin

Liberto de Pablo-Galán[1*], Juan J. de Pablo[2], and M. de Lourdes Chávez-García[3]

[1]*Instituto de Geología, Universidad Nacional Autonoma de México, México, D. F. 04510*
[2]*Chemical Engineering Department, University of Wisconsin-Madison, 1415 Engineering Drive, Madison, WI 53706*
[3]*Facultad de Química, Universidad Nacional Autonoma de México, México, D. F. 04510*
** e-mail: liberto@servidor.unam.mx*

ABSTRACT

Diagenesis of the Recent-Pleistocene volcanogenic depositional sequence of the Mexican Basin developed, in the gravel and sand strata, kaolinite, interstratified kaolinite/2H_2O-smectite, opal-C, 1H_2O- and 2H_2O-smectite and Si-contaminated smectite platelets, intimately associated with fine volcanic ash. The diagenesis initiated by silicification, sapropelic, in an environment of high permeability and hydraulic conductivity. At progressively higher depths, with decreasing permeability and flow, and higher alkalinity, kaolinite was transformed, via interstratified kaolinite/smectite, to 2H_2O-smectite platelets, and volcanic glass was directly transformed to smectite lamella. The mudstones are constituted by 2H_2O-smectite. In the smectite, cation replacement was in the tetra- and octahedral sheets, but the site of the charge is largely in the octahedral one. Layer charges vary between 0.2-0.9, some within the range of vermiculite. The clay minerals form across the sedimentary sequence a continuous non-uniform phase of heterogeneous composition and variable physical behavior that would influence the stability of the bulk sediments.

Keywords: diagenesis, mineralogy, clay mineralogy, stability, Mexican Basin.

RESUMEN

La diagénesis en la secuencia deposicional volcanogénica del Reciente-Pleistoceno de la Cuenca de México desarrolló, en los estratos de grava y arena, caolinita, interestratificados caolinita/2H_2O-esmectita, ópalo-C, plaquetas y laminas de 1H_2O- y 2H_2O-esmectita y de 2H_2O-esmectita contaminada con Si, íntimamente asociadas con ceniza volcánica fina. El proceso fue por silicificación, sapropélica, en ambiente de alta permeabilidad y conductividad hidráulica. A profundidades progresivamente mayores, con flujo y permeabilidad decrecientes, y alcalinidad creciente, la caolinita se transformó, vía interestratificados caolinita/esmectita, a plaquetas de 2H_2O-esmectita, y el vidrio volcánico formó directamente esmectita laminar. Las lodolitas están formadas por 2H_2O-esmectita. En la esmectita, el remplazamiento catiónico tuvo lugar en las hojas tetra- y octaédrica, pero el sitio de las cargas reside mayormente en la hoja octaédrica. Las cargas de las capas varían de 0.2-0.9, algunas dentro de los limites de vermiculita. Los minerales arcillosos forman a través de la secuencia sedimentaria una fase continua no uniforme, de composición heterogénea y comportamiento físico variable que incide en la estabilidad de los sedimentos.

Palabras clave: diagénesis, mineralogía, minerales arcillosos, estabilidad, Cuenca de México.

INTRODUCTION

Young volcanogenic sediments transform to mudrocks, frequently of non-uniform physical and chemical properties. Their behavior suggests that the diagenetic processes and the neoformed minerals could be heterogeneous across the sedimentary sequence. Aside from its basic interest, the characterization of their clay mineralogy and diagenesis is important to establish the correlation with older sediments; from the applications standpoint, the physical and chemical stability of sediments is relevant to rock mechanics, civil engineering and constructions, contamination of basin and aquifers, waste disposal, and many industrial applications. The uncontrolled and unpredictable stability of mudrocks may cause substantial and expensive damage. The physical instability and swelling of mudrocks are believed to be caused by the adsorption of water and chemical species and by electric-double layer phenomena on the expandable 2:1 clay minerals; in the extreme, swelling turns into fluidity. These expandable 2:1 clay minerals are the principal components in the lacustrine sediments of the Mexican Basin, where urban Mexico City locates. Herefore, the present interest on the study of the sediments and the interactions between the clay minerals and their physical and chemical behavior.

The physical and chemical stability problems in mudrocks and high-clay content sediments are usually managed assuming uniform behavior. However, their patterns of failure under load or under seismic events suggest that their behavior could be non-uniform, heterogeneous, which leads to postulate that variability in diagenesis and mineralogy would result in gradational differential behavior across the sedimentary sequence. In young sediments physical instability is the general rule. In old sediments, which tend to be stable, diagenesis is to trioctahedral smectite, Mg-rich chlorite, interstratified chlorite/smectite and corrensite, as occurs in intermediate to mafic volcanic rocks and volcanogenic sediments (Kubler, 1973; Almon *et al.*, 1976; April, 1981; Pevear and Whitney, 1982; Chang *et al.*, 1986; Inoue and Utada, 1991; Jiang and Peacor, 1994), marine evaporites (Bodine and Madsen, 1987), lacustrine mudrocks (April 1981; Hillier 1993; Barrenechea *et al.*, 2000), evaporitic sequences (Kopp and Fallis, 1974), and mafic intrusions (Furbish, 1975). Between the low-temperature smectite and the high-temperature chlorite exists a sequence of interstratified chlorite/smectite mixed-layers and corrensite (Hutcheon *et al.*, 1980; Meunier *et al.*, 1988; Hillier, 1993; Jiang and Peacor, 1994; Jiang *et al.*, 1994). The transformation of smectite to corrensite to chlorite has been described as continuous, characterized by random and regular interstratifications (April, 1981; Bettison-Varga and Mackinnon, 1997) and as a series of discontinuous steps (Roberson, 1989; Shau *et al.*, 1990; Hillier and Velde, 1991; Hillier, 1993; Schiffman and Staudigel, 1995).

The diagenesis of young sediments has not been completely documented, although the transformation of volcanogenic sediments to smectite is ubiquitously accepted. Associated with the smectite may occur 7Å-layer minerals, some of which have been loosely referred to as 7Å-chlorite, serpentine-like 7Å-layers, 7Å-layer or 7Å-clay (Karpova, 1969; Jiang *et al.*, 1994). Karpova (1969) described a Fe-7Å Ib(β 90º) chlorite that transforms to Fe-14Å Ib(β 90º) chlorite to Mg-Fe-14Å Iib chlorite, by burial diagenesis in terrigenous Carboniferous rocks. This Fe-7Å chlorite could correspond with a high-Fe-14Å chlorite or any of the 7Å high-Fe minerals chamosite, berthierine or even odinite (Brindley, 1982; Bailey and Brown, 1982; Odin, 1985; Odin *et al.*, 1988; Bailey, 1988a, 1988b). It could be presumed that, as in the case of the trioctahedral smectite, diagenesis of volcanoclastic sediments to 7Å-layer minerals or to dioctahedral smectite could be associated with interstratified 7Å-layer/smectite mixed-layers or even with chlorite, distinct from those developed under more intense stages of diagenesis. A logical postulate would be to expect dissimilar mechanisms of diagenesis and mineral assemblages within the pores and channels of gravel and sands and in the less permeable fine ash and mudstones. From the standpoint of the stability, the 7Å-layer minerals should modify to some extent the behavior of the sediments, which would still depend on the properties of their principal clay component, smectite. Based on the anomalous behavior of young sediments, it may be postulated that variations in the precursor minerals or in their diagenesis would result in distinct clay minerals, unevenly distributed through a sedimentary sequence, of non-uniform behavior.

This paper will document the occurrence and distribution of clay minerals, and diagenesis in the volcanogenic sediments of the Recent-Pleistocene depositional sequence of the Mexican Basin, Central Mexico, and their significance to their physical behavior.

GEOGRAPHIC AND GEOLOGIC SETTING

The Mexican Basin extends between the 19º00' and 20º15' N latitude and 98º15' and 99º33' W longitude, covering an area of 7,160 km^2 in central Mexico (Figure 1). The Basin was formed in the Middle Tertiary, when active volcanism developed thick sequences of basaltic andesite, andesite, dacite and latite; the sequence includes the dacitic and rhyolitic lavas of the Cerro del Chiquihuite, the andesite flows of the Sierras Nevada and Las Cruces, and the andesitic series of the Iztaccihuatl and the Ajusco Volcanoes. Volcanic activity decreased towards the end of the Miocene. Tectonism associated with the Clarion fault disrupted the crust along NNW-SSE fractures. During the Pliocene, intensive rains created the abrupt relief of the Middle and Upper Tertiary volcanic complexes and formed extensive flu-

vial deposits intercalated with strata of siltstone, lava flows and tuffs, with lenses of limestone (Tarango Formation). In the Pleistocene, the climate was humid and cold (Mooser, 1956; López-Ramos, 1979), glaciers developed in the Iztaccihuatl and Popocatepelt Volcanoes, and large portions of the Tarango Formation were destroyed. The area was covered with thick layers of basalt and pumice (Chiconautla, Chimalhuacan and Estrella) until intense lava effusions from the Sierra de Chichinautzin, 2,000 m thick, closed the drainage at the south end of the Basin. This was followed by an intense deposition of air and water transported ashes that settled in the low areas forming the Tacubaya Formation. The formation is characterized by intercalated strata of pyroclastic sands and ashes that in the lacustrine environment were transformed into the high swelling clays common to the Basin. Overlying the Tacubaya Formation are the lacustrine sediments of the Becerra Formation. The final eruptions were those of the Xitli about 2,400 years ago and of the Popocatépetl in 1920 (Mooser, 1956; Gasca and Reyes, 1977; López-Ramos, 1979; Sistema Hidráulico del Distrito Federal, 1994).

A simplified stratigraphic column of the Mexican Basin, which will be referred to simply as the Basin, will show a randomly distributed layered sequence of silt, mud, sand and gravel (Figure 2). The thickness of the mud is 100 m southeast of the Basin, in Xochimilco and Chalco, and northeast, in Texcoco. It ranges from 60 to 100 m to the northwest, in Atcapotzalco, and in the remaining areas averages from 40 to 60 m. The sediments described are from the Recent-Pleistocene Barranco and Tacubaya Formations, from locations in the north (Charcos) and south (Tezonco) of the Basin.

The mud retains large amounts of water, forms gels that liquefy easily, is mechanically unstable, highly compressible, of fine particle size and swells substantially

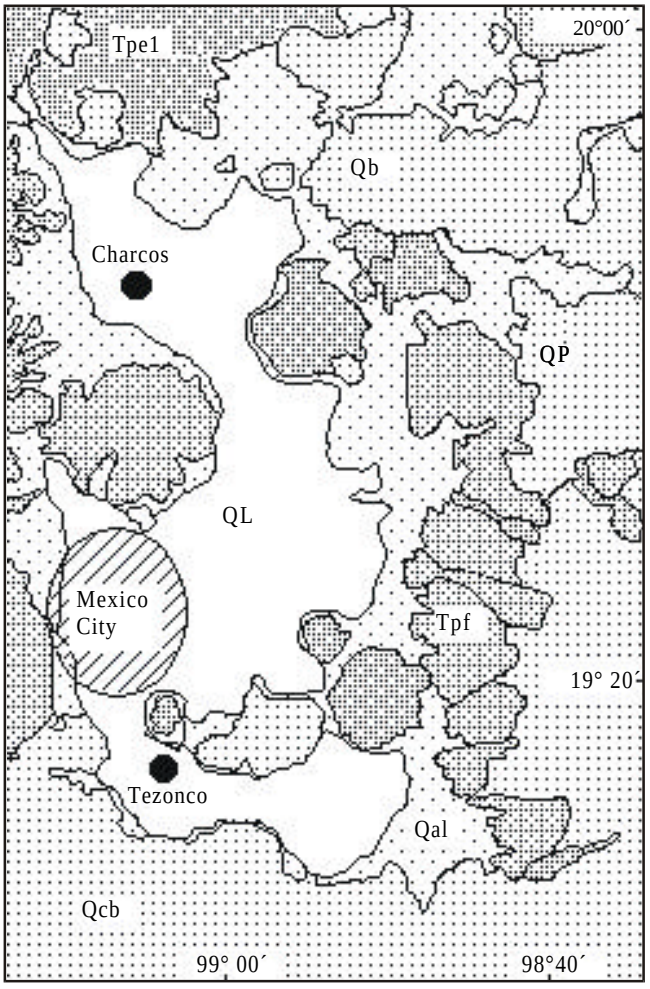

Figure 1. Geologic map of the Mexican Basin. QL, Quaternary lacustrine deposits; Qal, Quaternary alluvial deposits; Qcb, Quaternary lavas and tuffs of the Chichinautzin Group, basaltic; Qb, Quaternary Recent lavas; QP, Quaternary Pliocene basaltic lavas and tuffs older than the Chichinautzin Group; Tpf, Tertiary volcanic fans of the Tarango Formation; Tpel, Tertiary tuffaceous and pumicitic soils (from Mooser, 1956; Sistema Hidráulico del Distrito Federal, 1994).

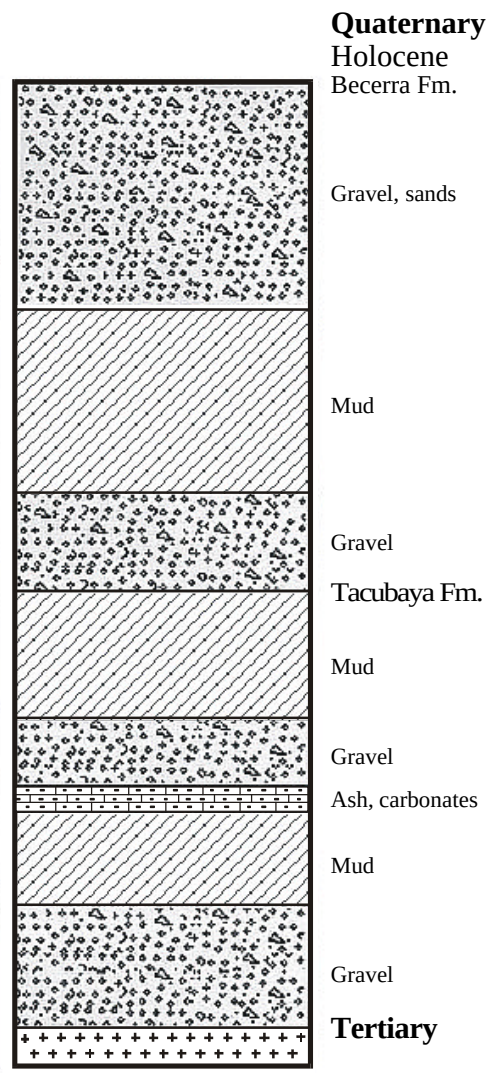

Figure 2. Schematic stratigraphic column of the Mexican Basin (data from Mooser, 1956; López-Ramos, 1979; Sistema Hidráulico del Distrito Federal, 1994).

(Marsal and Mazari, 1962). Other studies have described the hydrogeology (Durazo and Farvolden, 1989), stratigraphy and paleoenvironment of the southeastern part of the Basin (Urrutia-Fucugauchi *et al.*, 1994) and the distribution of heavy metals (Ruiz-Fernández, 1999). The clay has been described as bentonitic but its mineralogy, swelling, instability and other properties have not been adequately resolved. It is the purpose of this paper to establish the clay mineralogy and diagenesis and their possible influence on the stability of the sediments, hypothesizing on their behavior.

SAMPLING AND METHODOLOGY

The sediments studied were sampled from more than 20 drillholes extending over the Basin down to depths of 324 m. Two holes, located to the north (Charcos) and south (Tezonco) of the Basin and represented by 155 samples each were selected to document this presentation, and 17 of them were chosen to illustrate it. They are black to brown mudstones with variable contents of sand and ash, and gravel and sands with volcanoclastic gravel-size fragments, lapilli, sand and ash. The average properties of the mudstones had been described as water content 400 wt. %, liquid limit 1-70, plastic limit 30-80, cation exchange capacity 70 meq/100 g, deformation modulus 10.60 k/cm^2 when containing 50-600 wt. % water and compressive modulus 2-8 k/cm^2 (Marsal and Mazari, 1962).

The samples were prepared by dispersion in deionized water, screening and sedimentation of the fine silt and sand. Fractions of <2 μm and <0.5 μm were separated by gravity settling and centrifugation, adding the minimum water to avoid jellying. Samples for X-ray diffraction studies were prepared by dropping the suspended clay a few drops at a time on glass slides until a translucent layer had built. Analysis were done in a D5000 Siemens diffractometer, CuKα radiation, scanning at 1 º2θ/min from 2 to 65 º2θ and at 0.5 º2θ/min from 2 to 45 º2θ. Experimental patterns of the mixed-layer minerals were compared with those calculated with NEWMOD (Reynolds and Reynolds, 1996). However, the poor resolution shown by the interstratified minerals in the region between 2 and 15º 2θ and the similarities between them did not allow a simple straight identification. Smectite and vermiculite were differentiated by diffraction of samples saturated with Mg and glycerol. The 7Å-layer mineral was identified by its 001, 002 and 003 reflections that are unshifted by glycol and by the absence of the 14 Å chlorite peak. The volcanic glass was characterized by broad diffraction bands extending between 10-14 º2θ and 20-30 º2θ.

Morphology and chemical composition were studied by scanning electron microscopy (SEM) coupled with energy dispersive X-ray fluorescence spectrometry (EDXRF), on fractured surfaces and on <2 μm and <0.5 μm sediment fractions freeze-dried and sputtered with graphite. The EDXRF was calibrated with orthoclase, phlogopite, albite, and kaolinite reference samples. Structural compositions were calculated respectively for the $O_{10}(OH)_2$ half-cell of montmorillonite and the $(OH)_6$ cell of hydroxyl complexes (Güven, 1988; Bailey, 1988a, 1988b; Moore and Reynolds, 1997). Iron was calculated as Fe^{2+}.

RESULTS AND DISCUSSION

Upper strata of gravel and sand characterize the sedimentary sequence in the northern area of the Basin (Charcos), where clay is the minor component, intimately associated with fine ash. The ash contains volcanic glass, plagioclase, quartz, opal-C, K-feldspar and augite. Kaolinite, $1H_2O$- and $2H_2O$-smectite, and interstratified kaolinite/$2H_2O$-smectite mixed-layers occur in

Table 1. Mineralogy of the <2 mm fraction of sediments from the Mexican Basin.

Depth (m)	1H-S1	2H-S	K	KS	KF	Pl	Cr	C
			Charco					
8		XX	XX	X		X	X	
10	X	XX	XX	X		X		
16	XX		X	X	X	X		
18		XX	XX	X	X	X	X	
24		X	X	X	X	X	X	
26		XX	X	X	X	X	X	
86		XX	X	X	X	X	X	
88		X	X	X	X	X	X	
90	XX	X				X	X	
92	XX	XX	X	X			X	
148		XX	X		X	X	X	X
178	X	XX	X	X		X	X	X
188		XX		X	X	X	X	X
218		XX	X	X		X	X	
230		XXX	X	X		X	X	
254	XXX		X		X		X	
262	XXX	XX	X	X	X		X	
318	XX	XXX	X	X	X		X	
324	XXX	XXX	X	X	X	X	X	
			Tezonco					
14		XXX	X				X	
30		XXX	X				X	
60		XXX	X	X	X	X	X	
68		XX	XX	X	X	X	X	
102	X			XX	X	X	X	
262		X	XX		X	X	X	
284	X	X	XX				X	
286	X	X		XX	X	X	X	

Abbreviations: 1H-S: $1H_2O$-smectite; 2H-S: $2H_2O$-smectite; K: kaolinite; KS: interstratified kaolinite/smectite; KF: K-feldspar; Pl: plagioclase; Cr: cristobalite; C: calcite. The relative abundance of minerals is indicated by XXX when most abundant and X when least abundant.

the gravel and sand strata (Table 1). The minerals are dioctahedral, *d*(060) 1.496-1.50 Å, but occasional weak reflection at 1.52 Å, indicative of trioctahedral minerals, were recorded.

Volcanic glass, $2H_2O$-smectite, kaolinite, interstratified kaolinite/$2H_2O$-smectite, cristobalite and plagioclase are recognized at 18 m depth (Figure 3A, Table 1). The $2H_2O$-smectite is relatively less abundant than kaolinite; adsorption of ethylene glycol permitted differentiation of kaolinite from smectite and the interstratified minerals. At 26 m prevails the same mineralogy (Figure 3B). At 86 and down to 92 m (Figures 3C, 3D and 3E) the minerals are essentially the same, but $1H_2O$- and $2H_2O$-smectite tend to be more abundant whereas the non-clay minerals, including volcanic glass, decrease. A better separation of the clay minerals from the glass appears to occur at these depths. At 188 m (Figure 4A), the diffraction pattern is similar to that of the 92 m sediment (Figure 3E), except by the occurrence of calcite and fine-grained plagioclase, K-feldspar and cristobalite. At 262 m (Figure 4B) and down to 324 m (Figures 4C and 4D), $1H_2O$- and $2H_2O$-smectite are clearly predominant over volcanic glass, associated with minor interstratified kaolinite/smectite mixed-layers.

The mineralogical sequence is reversed in the southern area of the Basin (Tezonco) where 46 m, from 14 to 60 m (Figures 5A, 5B, and 5C), of overlying mud-

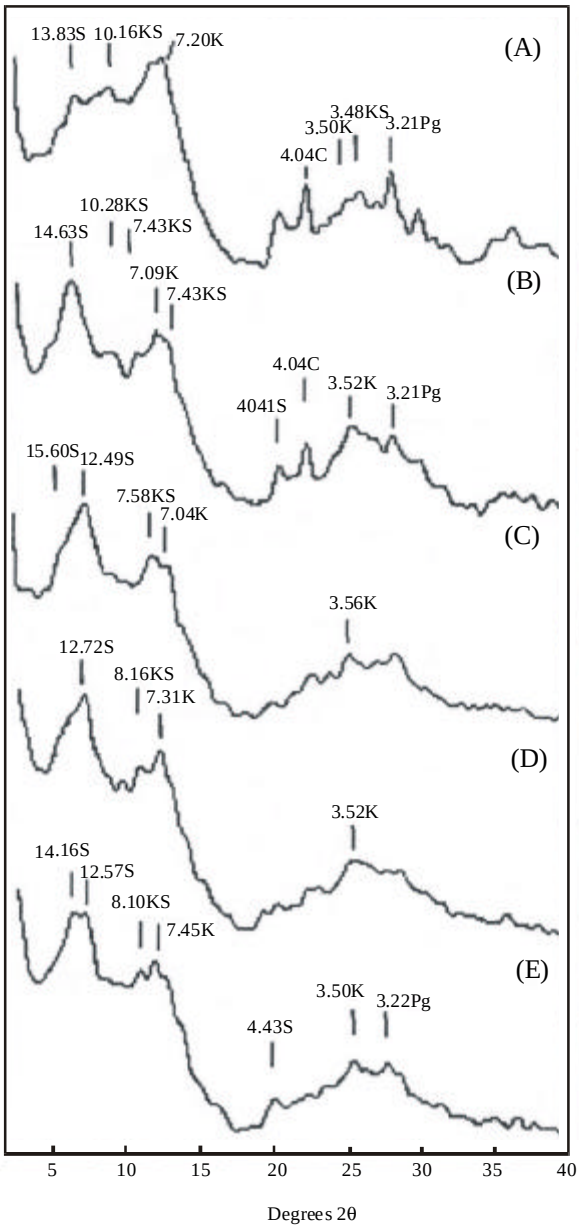

Figure 3. X-ray diffraction patterns of the <2 μm fraction (Charcos) of: (A) 18 m deep; (B) 26 m; (C) 86 m; (D) 90 m; (E) 92 m. S: smectite; K: kaolinite; KS: interstratified kaolinite/smectite; C: cristobalite; Pg: plagioclase; KF: K-feldspar.

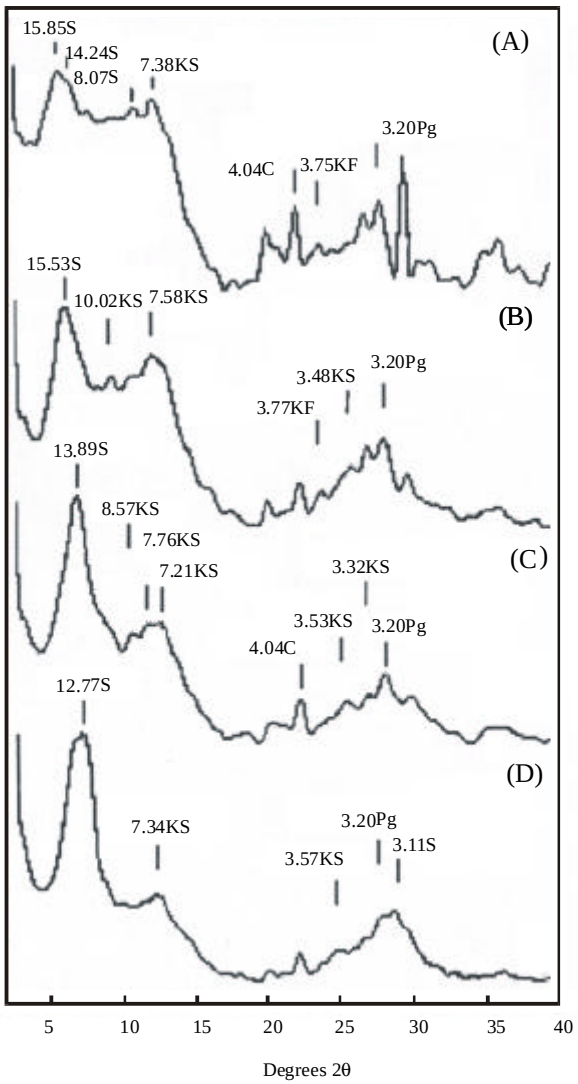

Figure 4. X-ray diffraction patterns of the <2 μm fraction (Charcos) of: (A) 188 m; (B) 262 m; (C) 318 m; (D) 324 m. For abbreviations see Figure 3.

stones formed essentially by $2H_2O$-smectite rest upon a thick 60-286 m strata of ash containing minor smectite, kaolinite, opal-C and interstratified kaolinite/smectite (Figures 5D, 5E, and 5F).

The morphology of the <2 µm fraction is characterized, at 10 m, by volcanic glass and glass transforming to hexagonal platelets (Figure 6A). At 86 m are recognized diatoms, glass shards, plagioclase, opal, glass transforming to hexagonal platelets and hexagonal platelets of smectite (Figures 6B), and, at 188 m, glass partially transformed to smectite and smectite lamella (Figure 6C).

Analyses by EDXRF of single fragments and crystals selected by SEM indicate predominance of opal in the upper strata. Opal averages 85 wt. % SiO_2 and minor Al_2O_3, FeO, MgO, CaO, Na_2O and K_2O (Table 2). It occurs associated with hexagonal platelets of silicified or Si-contaminated smectite that become less abundant at higher depths; their compositions are intermediate between those of opal and smectite (Table 3). Smectite is found at all levels, but is relatively more abundant at depth; it contains less than 65 wt. % SiO_2 and variable

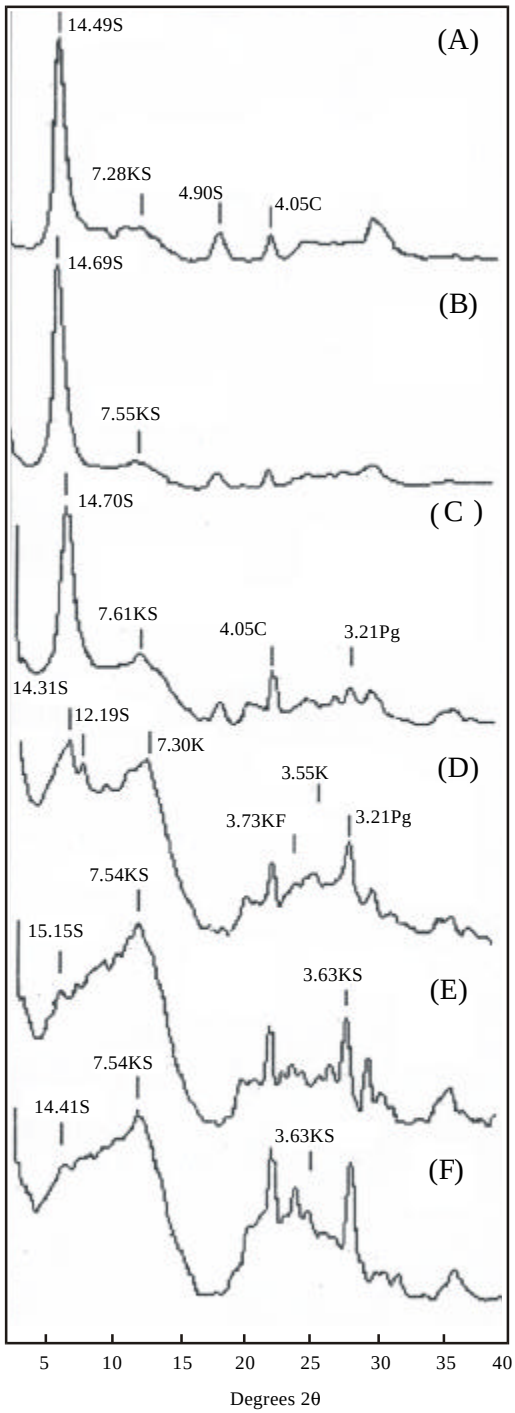

Figure 5. X-ray diffraction patterns of the <2 µm fraction (Tezonco) of: (A) 14 m; (B) 30 m; (C) 60 m; (D) 68 m; (E) 208 m; (F) 324 m. Abbreviations as in Figure 3

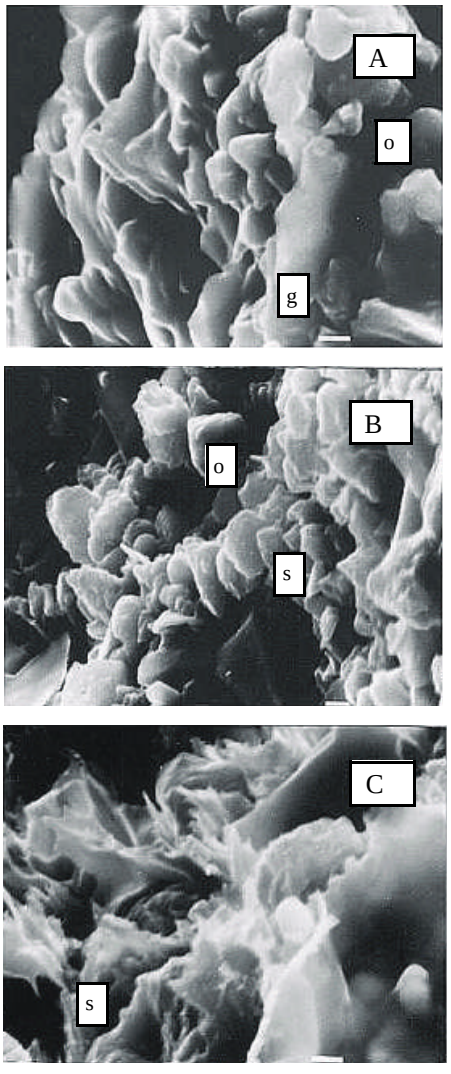

Figure 6. Scanning electron micrographs of the <2 µm fraction (Charcos) showing: (A), 10 m, glass, opal, glass partially transformed to hexagonal outlines; (B), 86 m, smectite platelets; (C), 188 m, smectite lamella and glass transforming to smectite. O, opal; g, glass; s, smectite. The horizontal bar represents 1 micron.l

Table 2. Chemical composition of opal-C.

	Charco										Tezonco			
Depth (m)	10	10	10	10	10	10	86	90	90	90	2	2	4	Average
Sample	5	6	12	15	17	20	81	24	25	27	60	63	77	
SiO_2 (wt. %)	84.97	88.21	88.56	82.15	84.32	88.59	92.3	83.95	84.52	82.27	83.98	82.36	84.83	85.45
TiO_2	0.03	0.55	0.16	1.08	0.54	0.45	0.58	0.95	0.33	0.83	0.36	0.63	0	0.5
Al_2O_3	8.75	6.36	6.97	11.6	9.72	6.99	3.91	7.4	8.13	9.88	8.44	10	8.1	8.17
FeO	1.56	1.02	1.69	2.85	2.44	1.19	2.05	4.06	3.88	3.38	2.77	1.97	3.68	2.5
MnO	0.27	0.01	0.23	0	0.31	0	0.06	0.51	0.38	0.12	0.34	0.23	0.11	0.2
MgO	0.69	0.61	0.94	0.89	0.85	0.59	0.37	1.23	1.74	1.68	1.61	2.38	1.54	1.16
CaO	1.27	0.8	0.56	0.22	0.8	0.55	0.12	1.3	0.57	0.48	0.88	0.82	1.49	0.76
Na_2O	0.8	0.74	0.64	0.45	0.5	0.61	0.52	0.11	0.17	0.8	0.6	0.43	0	0.49
K_2O	1.64	1.7	0.24	0.76	0.51	0.96	0	0.5	0.27	0.55	1.02	1.17	0.65	0.77

Analyses by EDXRF on fragments selected by SEM.

Al_2O_3, FeO and MgO (Table 4). Hydroxyl complexes of Al and Fe were identified at 16 m (Table 5). Opal, silicified smectite and smectite keep a lineal correlation between SiO_2 and Al_2O_3+TiO_2+FeO+MnO+MgO, indicative of diagenesis by silicification (Figure 7). The hydroxyl complexes also follow this correlation.

Smectite platelets and lamella have compositions (Table 4) that are grouped in: (1), aluminian, of high $^{VI}Al^{3+}$ and $^{IV}Al^{3+}$; (2), aluminian, of high $^{VI}Al^{3+}$; (3), ferrous, of relatively high tetrahedral $^{IV}Al^{3+}$ and octahedral Fe^{2+}; (4), magnesian, with substantial octahedral Mg^{2+}, and (5), intermediate, with octahedral $^{VI}Al^{3+}$, Fe^{2+} and Mg^{2+}. They indicate the occurrence of high $^{IV}Al^{3+}$-smectite leaning towards beidellite, of intermediate beidellite-nontronite, and of smectite tending to saponite, or to smectite/vermiculite mixed-layers. In smectite, the octahedral $^{VI}Al^{3+}$+Ti^{4+}+Fe^{2+}+Mn^{2+}+Mg^{2+} vary from 2.18 atoms per formula unit (afu) when tetrahedral substitution is 0.3 afu, to 2 afu when there is no tetrahedral replacement (Figure 8). Compositions that deviate positively from this average are rich in Fe^{2+} and Mg^{2+} whereas those of higher $^{VI}Al^{3}$ and lower (Fe^{2+}+Mg^{2+}) deviate negatively; silicified smectite platelets have Si^{4+}>4.

There is no significant correlation between octahedral Fe^{2+}+Mg^{2+} and tetrahedral $^{IV}Al^{3+}$ (Figure 9); the Fe/(Fe+Mg) ratio stays constant at about 0.55, not far from the 0.68 value that characterizes basalt (Morse, 1980; Cathelineau and Nieva, 1985). Smectite platelets of low Mg^{2+} and high Fe^{2+} deviate positively from the

Table 3. Chemical composition of Si-contaminated smectite.

	Charco														
Depth (m)	10	10	10	10	10	10	10	10	10	10	92	218	218	218	Average
Sample	14	9	16	18	19	22	23	37	40	41	82	42	50	51	
SiO_2 (wt. %)	70.55	73.37	69.95	71.49	75.26	77.74	73.56	73.66	70.95	77.27	71.21	70.85	71.82	71.17	73.15
TiO_2	0	0.43	0.85	0.12	0.21	0.45	0.61	0.82	0.77	0.29	0.92	0.35	0.73	0.41	0.44
Al_2O_3	15.89	15.75	17.54	20.57	15.28	13.79	15.68	17.51	20.02	13.89	17.4	17.36	12.73	8.64	16.22
FeO	3.49	2.54	7.14	4.39	4.46	3.48	6.46	2.59	2.09	2.17	6.01	3.8	8.94	3.12	3.69
MnO	0.11	0.15	0	0.16	0.07	0.73	0.09	0.12	0.03	0	0.11	0	0.5	0.33	0.14
MgO	0	1.18	1.55	1.13	2.29	1.55	1.16	1.49	3.74	5.15	1.61	1.11	3.01	13.77	1.75
CaO	8.41	0.45	1	0.75	1	0.66	0.93	1.01	0.88	0.3	0.94	3.02	1.23	0.67	2.36
Na_2O	0	0.94	0.76	0.65	0.52	0.7	0.45	0.76	1.06	0.77	0.77	1.69	0.25	0.73	0.7
K_2O	1.54	5.2	1.2	0.75	0.98	0.88	1.06	2.03	0.47	0.15	0.54	2.62	0.79	1.17	1.55
	Tezonco														
Depth (m)	2	2	2	2	2	2	2	3	3	3	218	218	218	218	Average
Sample	52	59	62	54	55	56	57	65	66	67	72	73	74	75	
SiO_2	78.06	78.37	78.54	68.99	68.02	69.47	69.77	69.28	68.51	68.3	67.13	66.21	68.36	67.48	70.46
TiO_2	0.27	0.11	0.15	3.29	0.87	0.16	0.35	0.35	0.43	0.97	1.15	0.83	0.7	0.18	0.7
Al_2O_3	12.27	12.22	12.07	15.4	18.1	17.1	23.01	18.02	17.55	16.86	14.1	13.65	18.02	17.1	16.1
FeO	3.92	3.02	3.18	6.16	5.76	5.71	3.29	3.08	3.73	5.42	12.63	8.8	4.78	5.76	5.37
MnO	0.13	0.04	0	0.03	0.13	0	0.18	0.25	0.23	0	0.04	0.09	0.23	0.09	0.1
MgO	2.84	3.12	2.71	2.74	4.45	4.27	1.64	5.82	5.87	4.47	1.95	4.12	4.06	5.05	3.79
CaO	0.68	1.12	1.57	1.58	1.02	1.37	1.28	1.19	1.26	2.22	1.88	1.47	1.32	1.09	1.36
Na_2O	0.76	1.05	0.56	1.02	0.37	0.41	0	1.34	1.4	0.91	0.23	1.98	0.36	0.36	0.77
K_2O	1.08	0.95	1.21	0.79	1.2	1.52	0.48	0.68	1.02	0.87	0.88	2.84	2.17	2.98	1.33

Analyses by EDXRF on platelets selected by SEM.

Table 4. Chemical compositions of smectite.

	Charco														
Depth (m)	10	10	10	10	10	86	86	90	90	90	90	90	90	92	218
Sample	7	34	35	36	39	79	80	27	28	29	30	31	32	84	43
SiO_2 (wt. %)	65.71	67.63	68.74	67.81	60.05	59.54	65.68	62.57	57.13	62.42	56.34	67.13	66.77	64.71	60.14
TiO_2	1.22	1.35	1.24	0.54	2.26	2.54	0.56	0.83	3.4	0.25	2.38	0.61	0.76	0.75	1.86
Al_2O_3	17.57	19.17	15.27	16.36	23.7	15.59	20.3	24.5	19.73	24.68	23.17	21.4	20.45	17.11	19.24
FeO	10.52	4.79	2.67	3.16	6.57	9.86	7.15	7.35	9.35	1.77	12.74	4.35	5.59	7	13.45
MnO	0.14	0.1	0.15	0.16	0.26	0.46	0.2	0.01	1.02	0.07	0.23	0	0.14	0.14	0.01
MgO	1.21	3.72	8.38	6.87	3.5	6.94	3.59	2.64	1.72	0.85	2.56	0.52	1.52	7.36	0.71
CaO	1.65	1.49	1.33	1.8	2.47	1.13	1.15	0.86	5.25	5.43	1.64	2.27	1.99	1.46	2.31
Na_2O	0.18	1.09	0.97	2.23	1.13	0.5	0.76	0.6	2.02	4.12	0.11	3.38	2.1	0.41	0.65
K_2O	1.79	0.66	1.25	1.09	0.06	3.42	0.69	0.64	0.38	0.41	0.83	0.34	0.67	1.06	1.64
Si^{4+}	4.06	4.05	4.1	4.07	3.67	3.78	3.97	3.79	3.63	3.78	3.56	4.03	4.02	3.95	3.81
Ti^{4+}	0.06	0.06	0.06	0.02	0.1	0.12	0.03	0.04	0.16	0.01	0.11	0.03	0.03	0.03	0.09
$^{IV}Al^{3+}$	0	0	0	0	0.33	0.22	0.03	0.21	0.37	0.22	0.44	0	0	0.05	0.19
$^{VI}Al^{3+}$	1.28	1.35	1.07	1.16	1.38	0.95	1.42	1.54	1.11	1.54	1.29	1.51	1.45	1.18	1.25
Fe^{2+}	0.54	0.24	0.13	0.16	0.34	0.52	0.36	0.37	0.5	0.09	0.67	0.22	0.28	0.36	0.72
Mn^{2+}	0.01	0.01	0.01	0.01	0.01	0.02	0.01	0	0.05	0	0.01	0	0.01	0.01	0
Mg^{2+}	0.11	0.33	0.75	0.62	0.32	0.66	0.32	0.24	0.16	0.08	0.24	0.05	0.14	0.67	0.07
Ca^{2+}	0.11	0.1	0.09	0.12	0.16	0.08	0.07	0.06	0.36	0.35	0.11	0.15	0.13	0.1	0.16
Na^{+}	0.02	0.13	0.11	0.26	0.13	0.06	0.09	0.07	0.25	0.48	0.01	0.39	0.25	0.05	0.08
K^{+}	0.14	0.05	0.1	0.08	0	0.28	0.05	0.05	0.03	0.03	0.07	0.03	0.05	0.08	0.13

	Charco					Tezonco					Smectite averages				
Depth (m)	218	218	218	218	218	2	2	4	218	218					
Sample	44	45	46	47	48	53	64	78	71	76	Al	Al	Fe	Mg	
SiO_2	61.65	61.88	61.37	62.35	66.62	66.05	65.32	59.52	66.05	64.74	57.84	63.73	60.16	65.2	65.19
TiO_2	2.02	0.99	1.01	0.31	1.1	0.54	0.13	2.54	0.96	0.91	2.68	0.9	2.46	1.27	1.01
Al_2O_3	17.62	24.9	23.43	23.65	18.03	17.77	19.59	15.62	20.98	20.81	22.2	22.69	16.63	16.08	19.03
FeO	11.2	6.8	7.05	2.18	5.19	4.33	4.98	9.86	7.67	6.56	9.55	5.64	9.89	5.67	6.31
MnO	0.11	0	0.22	0.07	0.45	0.45	0.02	0.46	0	0	0.5	0.12	0.5	0.23	0.21
MgO	4.26	2.61	4.28	2.22	2.45	4.45	5.9	6.95	2.18	3.42	2.59	2.28	5.12	7.39	4.08
CaO	1.46	1.05	0.89	5.3	3.73	4.05	1	1.13	0.84	1.31	3.18	2.16	1.9	1.43	1.84
Na_2O	0.73	1.02	1.16	3.69	2.19	0.63	1.16	0.51	0.61	0.92	1.08	1.74	0.71	1.03	0.98
K_2O	0.76	0.76	0.6	0.25	0.24	1.73	2	3.42	0.71	1.33	0.42	0.73	2.64	1.71	1.35
Si^{4+}	3.85	3.75	3.74	3.78	4.04	4.01	3.95	3.78	3.99	3.93	3.62	3.86	3.8	3.98	3.96
Ti^{4+}	0.1	0.05	0.05	0.01	0.05	0.02	0.01	0.12	0.04	0.04	0.13	0.04	0.12	0.06	0.05
$^{IV}Al^{3+}$	0.14	0.25	0.26	0.22	0	0	0.05	0.22	0.01	0.07	0.38	0.14	0.2	0.02	0.04
$^{VI}Al^{3+}$	1.16	1.53	1.42	1.47	1.29	1.27	1.35	0.95	1.49	1.42	1.26	1.48	1.04	1.14	1.32
Fe^{2+}	0.45	0.35	0.36	0.11	0.26	0.22	0.25	0.52	0.39	0.33	1	0.29	0.52	0.29	0.32
Mn^{2+}	0.01	0	0.01	0	0.02	0.02	0	0.02	0	0	0	0.01	0.03	0.01	0.01
Mg^{2+}	0.4	0.24	0.39	0.2	0.22	0.4	0.53	0.66	0.2	0.31	0.24	0.21	0.48	0.67	0.37
Ca^{2+}	0.1	0.07	0.06	0.34	0.24	0.26	0.06	0.08	0.05	0.09	0.21	0.14	0.13	0.09	0.12
Na^{+}	0.09	0.12	0.14	0.43	0.26	0.07	0.14	0.06	0.07	0.11	0.13	0.2	0.09	0.12	0.12
K^{+}	0.06	0.06	0.05	0.02	0.02	0.13	0.15	0.28	0.05	0.1	0.03	0.06	0.21	0.13	0.1

Analyses by EDXRF on lamella selected by SEM.

average whereas those of high Mg^{2+} do it negatively. Substitution in the octahedral sheet between R^{3+} and R^{2+} atoms shows a lineal inverse correlation (Figure 10) between low $^{VI}Al^{3+}$ and Fe^{2+} or high Mg^{2+} compositions and those of high $^{VI}Al^{3+}$ and Fe^{2+}.

The adsorbed cations $Ca^{2+}+Na^{+}+K^{+}$ attain a nearly uniform value of 0.25 afu, independent of replacement in the tetrahedral sheet of ^{IV}Si by $^{IV}Al^{3+}$ (Figure 11). However, they descent linearly with increasing saturation of the octahedral sheet by $^{VI}Al^{3+}+Ti^{4+}+Fe^{2+}+Mn^{2+}+Mg^{2+}$ (Figure 12). The highest adsorption is shown by aluminian smectite, of high $^{IV}Al^{3+}$ and $^{VI}Al^{3+}$, and the lowest by those rich in Fe^{2+} and Mg^{2+}. The compositions of the octahedral sheet vary between those of high-layer charge high-Al smectite, and those Fe- and Mg-smectite of lower charge and adsorption (Figure 12). The adsorbed cations range between 0.2-0.9 afu that correspond with layer charges of 0.24-1.15 equivalents (Table 4). The majority of the layer charges are within the 0.2-0.6 limits accepted for montmorillonite, but some are within the range of 0.6-0.9 equivalents of vermiculite (Suquet *et al.*, 1975, 1977; Güven, 1988). At these high values, there is no difference in the stability of the layers (Mering and Pedro, 1969; Suquet and Pezerat, 1987, 1988). Three compositions that have high $^{VI}Al^{3+}$, $^{IV}Al^{3+}$ and Fe^{2+}, show anomalous high layer charges between 1.00-1.15 equivalents that could possibly correspond with smectite/vermiculite interstratifications or with hydroxyl complexes adsorbed on smectite.

Table 5. Compositions of hydrooxyl complexes.

Depth (m)	16	16
Sample	69	70
SiO_2 (wt. %)	0	0
TiO_2	2.87	2.16
Al_2O_3	64.6	66.98
FeO	10	15.91
MnO	1.62	0
MgO	7.15	5.31
CaO	6.69	2.91
Na_2O	5.1	2.72
K_2O	1.97	4.01

Analyses by EDXRF on lamella selected by SEM.

Diagenesis appears in the strata of gravel and sand as a process of silicification, sapropelic, by which organic acids removed Si^{4+} from diatoms, K-feldspar, pyroxene and plagioclase, enriching the fluid in Si^{4+}, K^{+}, Na^{+}, Ca^{2+} and Mg^{2+} and crystallizing kaolinite. Volcanic glass was transformed to smectite and silicic acid to opal-C. The process prevailed in the strata of gravel and sand (upper 86 m, Charcos) were organic acids were abundant, and permeability and hydraulic conductivity were high. With increasing depth, kaolinite was transformed to smectite via interstratified kaolinite/smectite, as the composition of the fluid changed towards alkalinity and permeability and flow became increasingly limited. Conditions of drought and falling lake level prone to kaolinization (Hower *et al.*, 1976; April, 1981) could have developed. The hydroxyl complexes recognized at 16 m presumably resulted from kaolinite. In the mudstones (86-324 m, Charcos), volcanic ash was almost totally transformed to smectite in an alkaline environment of very low permeability and almost stagnant flow, with local variations in composition that resulted in smectite of different Mg/Fe ratios. Smectite was formed from: (1), volcanic glass and plagioclase in the high-silicic acid, low-pH, high-permeability and hydraulic conductivity environment of the gravel and sand strata; (2), volcanic glass in the alkaline, low-permeability environment of the mudstones; (3), kaolinite via interstratified kaolinite/smectite.

The 7Å-layered mineral recognized in the Basin is kaolinite. Other 7Å minerals like berthierine $(R^{2+}{}_aR^{3+}{}_b\ddot{y}_c)(Si_{2-x}Al_x)O_5(OH)_4$, odinite or chlorite were not observed. Berthierine has 0.45 to 0.90 ^{IV}Al afu and, in the octahedral sheet, contains R^{3+} between 0.37-1.03 Al^{3+} plus 0.1-0.27 Fe^{3+} and R^{2+} between 1.33-1.84 Fe^{2+} plus 0.08-0.66 Mg^{2+}. Odinite accommodates 0-0.20 ^{IV}Al afu, and in the octahedral sheet has Fe^{3+} 0.7-1.0 atoms and Mg as the main R^{2+} cation (Brindley, 1982; Arima *et al.*, 1985; Odin, 1985; Odin *et al.*, 1988; Bailey, 1988a, 1988b). Compositions that could indicate chlorite were not recorded (Foster, 1962; Bailey, 1988b; Caritat *et al.*, 1993).

Illite was not recognized, although the occurrence of very minor K-feldspar and presumably of mica suggested the possibility of finding it. If there was any, it would have possibly transformed to smectite (Rimmer and Eberl, 1982; Willman *et al.*, 1989; Moore and Reynolds, 1997) or to kaolinite through the sequence K-feldspar → smectite → smectite + illite → illite → illite + kaolinite → kaolinite → kaolinite + gibbsite → gibbsite (Hutcheon, 1980; Caritat *et al.*, 1993). The smectite → illite burial diagenesis at 110-100ºC (Hower *et al.*, 1976; Chang *et al.*, 1986; Weaver, 1989) did not develop. The $^{IV}Al^{3+}$ of smectite (Table 5) did not reach the

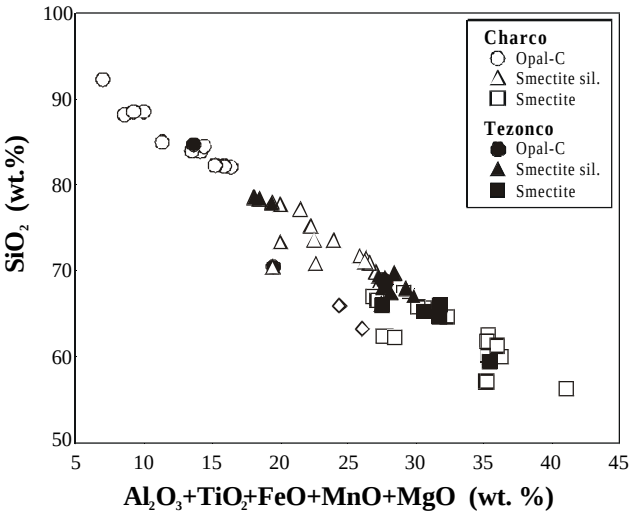

Figure 7. Correlation between the SiO_2 and $Al_2O_3+TiO_2+FeO+MnO+MgO$ components of smectite, Si-contaminated smectite and opal-C. The correlation is indicative of diagenesis by silicification.

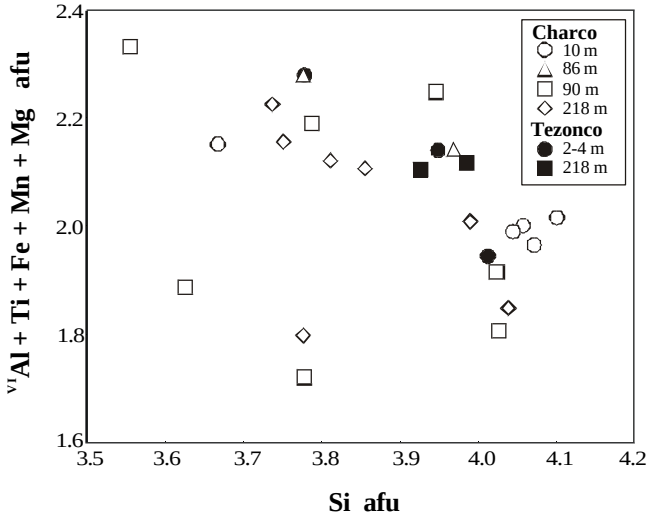

Figure 8. Correlation between the tetra- and octahedral sheets in smectite. $^{IV}Si>4$ corresponds with Si-contaminated smectite platelets.

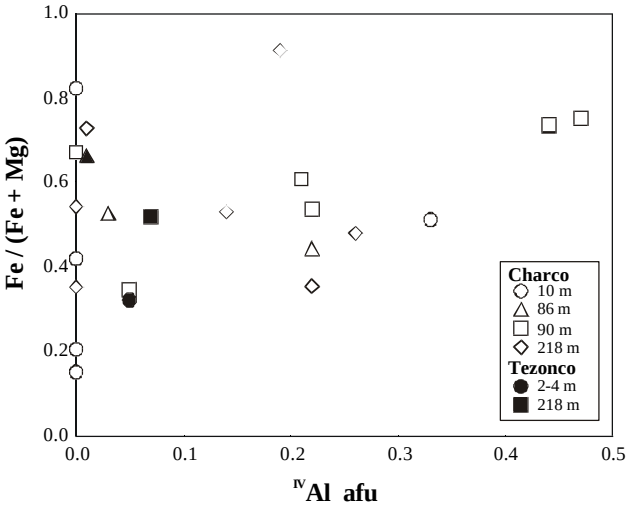

Figure 9. Correlation between the tetrahedral ^{IV}Al and the octahedral Fe/(Fe+Mg) ratio of smectite.

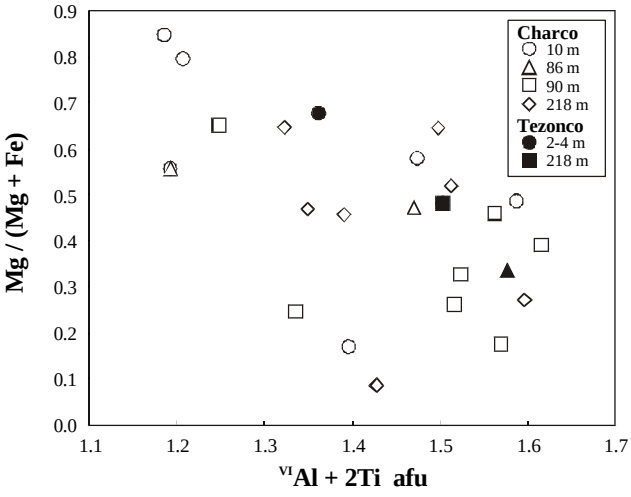

Figure 10. Correlation between the octahedral (VIAl+2Ti) cations and the Mg/(Mg+Fe) ratio of smectite.

0.5 afu expected for illite. Chlorite did not formed. The reported crystallization of saponite through chlorite/ smectite and corrensite (Sudo *et al.*, 1954; Sudo and Kodama, 1957; Almon *et al.*, 1976; Seyfried *et al.*, 1978; Hoffman and Hower, 1979; Chang *et al.*, 1986; Roberts and Merriman, 1990) was not recognized. The reactions of illite, kaolinite or berthierine with M^{2+}-rich fluids to smectite to chlorite (April, 1981; Vergo and April, 1982; Ahn and Peacor, 1985; Chang *et al.*, 1986; Weaver, 1989; Walker and Thompson, 1990; Inoue and Utada, 1991; Jiang and Peacor, 1994), or between dolomite, illite and quartz to calcite and chlorite (Almon *et al.*, 1976; Hutcheon *et al.*, 1980; Hillier, 1993; Barrenechea *et al.*, 2000) were not observed. The transformations from Ib(b90º) Fe 7Å-chlorite to regular Ib(b90º) Fe 14Å-chlorite (Karpova, 1969), of chlorite polytypes Ibd Ibd(b97º) Ib(b90º) Iib (Hayes, 1970), or of IIb chlorite from berthierine (Fe/Fe+Mg>0.8) (Curtis *et al.*, 1985) did not occur. The smectite in the Basin has compositions far from those of ^{IV}Si~3.25, 0.4<Fe/(Fe+Mg) <0.7, 0.4-0.8 (^{IV}Al-1), 0-0.6 (^{VI}Al+2Ti+Cr-1) common to chlorites (Curtis *et al.*, 1985; Laird, 1988; Hillier and Velde, 1991; Jahren and Aagaard, 1992; Caritat *et al.*, 1993). The smectite-chlorite transformation, which would improve the chemical and physical stability of the sediments, did not developed.

The clay minerals form a fine continuous phase that extends through the sedimentary sequence, ranging from minor smectite, kaolinite and interstratified kaolinite/smectite in the upper gravel and sand strata, through decreasing kaolinite and interstratified minerals and increasing smectite in the lower strata, to abundant smec-

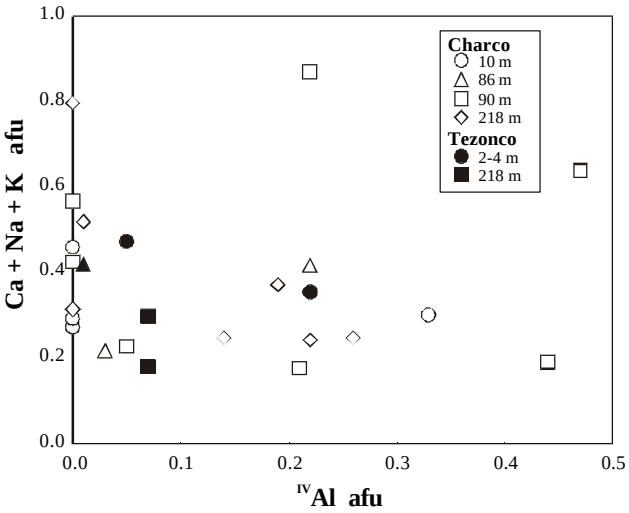

Figure 11. Correlation betwen the adsorbed cations and the tetrahedral replacement in smectite.

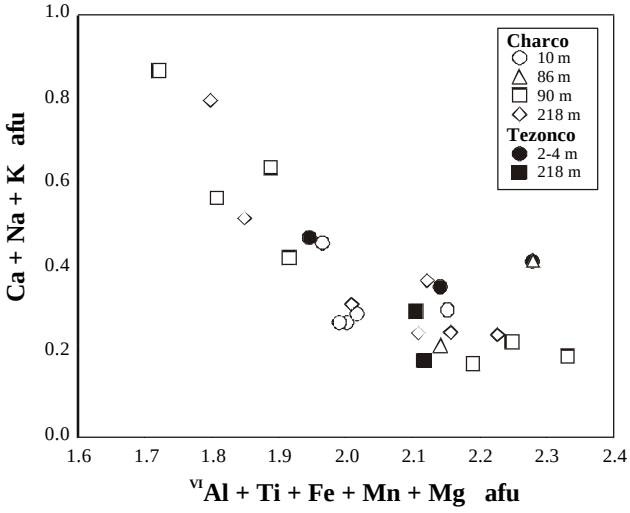

Figure 12. Correlation between the adsorbed cations and the octahedral sheet of smectite.

tite in the mud. The increasingly abundance of clay minerals with depth, their progressive transformation to smectite, and the variable composition of the smectite platelets and lamella, convey to their non-uniform heterogeneous distribution across the sedimentary sequence. The properties and behavior of the clay fraction would not be the same horizontally and vertically across the sequence. Much to the contrary, a non-uniform heterogeneous behavior is expected for the clay minerals and for the fine and coarser fraction of the sediments. The prevalence of dioctahedral smectite minerals define a physically and chemically unstable system, opposed to the less expandable more mechanically stable trioctahedral smectite-chlorite systems known to occur in old sedimentary sequences (Chang *et al.*, 1986; Jiang and Peacor, 1994).

CONCLUSIONS

Low-grade diagenesis of the Recent-Pleistocene volcanogenic sequence of the Mexican Basin developed opal-C, kaolinite, dioctahedral $1H_2O$- and $2H_2O$-smectite, interstratified kaolinite/smectite, and Si- or glass-contaminated smectite, in an environment of high permeability and hydraulic conductivity, rich in organics. With increasing depth, decreasing permeability and hydraulic conductivity, increasing fluid alkalinity, kaolinite was transformed via interstratified kaolinite/smectite to $2H_2O$-smectite, and volcanic glass was directly to smectite lamella. The clay minerals form a fine, continuous, non-uniform phase of variable composition, morphology, and abundance, of heterogeneous behavior. Although the clay fraction represents 3-20 wt. % in the gravel and sand strata to over 85 wt. % in the mudrocks, its behavior would certainly affect that of the bulk sediments.

ACKNOWLEDGEMENTS

The authors acknowledge the financial support of the Consejo de Ciencia y Tecnología and the National Science Foundation, grant 400324-CO46A. They are indebted to the Dirección General de Construcción y Operación Hidráulica, Departamento del Distrito Federal, for supplying material for study and pertinent data, and to Víctor Malpica. They manifest their appreciation to A. Altamira, L. Cabrera, A. Maturano and M. Reyes for their contribution.

REFERENCES

Ahn, J.H., Peacor, D.R., 1985, Transmission electron microscopic study of diagenetic chlorite in Gulf Coast argillaceous sediments: Clays and Clay Minerals, 33, 228-236.

Almon, W.R., Fullerton, L.B., Davies, D.K., 1976, Pore space reduction in Cretaceous sandstone through chemical precipitation of clay minerals: Journal of Sedimentary Petrology, 46, 89-96.

April, R.H., 1981, Trioctahedral smectite and interstratified chlorite/smectite in Jurassic strata of the Connecticut Valley: Clays and Clay Minerals, 29, 31-39.

Arima, M., Fleet, M., Barnett, R.L., 1985, Titanian berthierine: a Ti-reach serpentine group mineral from the Picton ultramafic dyke, Ontario: Canadian Mineralogist, 23, 213-220.

Bailey, S.W., 1988a, Structures and composition of other trioctahedral 1:1 phyllosilicates, *in* Bailey, S.W. (ed.), Hydrous phyllosilicates: Washington, D.C., Mineralogical Society of America, Reviews in Mineralogy, 19, 169-188.

Bailey, S.W., 1988b, Chlorites: Structure and crystal chemistry, *in* Bailey, S.W. (ed.), Hydrous phyllosilicates:Washington, D.C., Mineralogical Society of America, Reviews in Mineralogy, 19, 347-404.

Bailey, S.W., Brown, B.E., 1982, Chlorite polytypism: I. Regular and semi-random one-layer structures: American Mineralogist, 47, 819-850.

Barrenechea, J.F., Rodas, M., Frey, M., Alonso-Azcarate, J., Mas, J.R., 2000, Chlorite, corrensite, and chlorite-mica in late Jurassic fluvio-lacustrine sediments of the Cameros Basin of Northeastern Spain: Clays and Clay Minerals, 48, 256-265.

Bettison-Varga, L., Mackinnon, I.D.R., 1997, The role of randomly mixed-layered chlorite/smectite in the transformation of smectite to chlorite: Clays and Clay Minerals, 45, 506-516.

Bodine, M.W., Madsen, B.M., 1987, Mixed-layer chlorite/smectites from a Pennsylvanian evaporite cycle, Grand County, Utah, *in* Schultz, L.G., van Olphen, H., and Mumpton, F.A. (eds.), Proceedings of the International Conference, Denver, 1985: Denver, The Clay Minerals Society, p. 85-93.

Brindley, G.W., 1982, Chemical composition of berthierine –a review: Clays and Clay Minerals, 30, 153-155.

Caritat, P. de, Hutcheon, I., Walshe, J.L., 1993, Chlorite geothermometry: a review: Clays and Clay Minerals, 41, 219-239.

Cathelineau, M., Nieva, D., 1985, A chlorite solid solution geothermometer. The Los Azufres (Mexico) geothermal system: Contributions to Mineralogy and Petrology, 91, 235-244.

Chang, H.K., Mackenzie, F.T., Schoonmaker, J., 1986, Comparisons between the diagenesis of dioctahedral and trioctahedral smectite Brazilian offshore basins: Clays and Clay Minerals, 34, 407-423.

Curtis, C.D., Hughes, C.R., Whiteman, J.A., Whittle, C.K., 1985, Compositional variations within some sedimentary chlorites and some comments on their origin: Mineralogical Magazine, 49, 375-386.

Durazo, J., Farvolden, R.N., 1989, The groundwater regime of the Valley of Mexico from historic evidence and field observations: Journal of Hydrology, 112, 171-190.

Foster, M.D., 1962, Interpretation of the composition and a classification of the chlorites: United States Geological Survey, Profesional Paper, 414-A, p. 1-33.

Furbish, W.J., 1975, Corrensite of deuteric origin: American Mineralogist, 60, 928-930.

Gasca, D.A., Reyes, C.M., 1977, La cuenca lacustre Plio-Pleistocénica de Tula-Zumpango: México, Instituto Nacional Antropología e Historia, Informe, 2, 1-85.

Güven, N., 1988, Smectites, *in* Bailey, S.W. (ed.), Hydrous phyllosilicates: Washington, D.C., Mineralogical Society of America, Reviews in Mineralogy, 19, 497-559.

Hayes, J.B., 1970, Polytypism of chlorite in sedimentary rocks: Clays and Clay Minerals, 18, 285-306.

Hillier, S., 1993, Origin, diagenesis and mineralogy of chlorite minerals in Devonian Lacustrine mudrocks, Orcadian Basin, Scotland: Clays and Clay Minerals, 41, 240-259.

Hillier, S., Velde, B., 1991, Octahedral occupancy and the chemical composition of diagenetic (low-temperature) chlorites: Clay Minerals, 26, 149-168.

Hoffman, J., Hower, J., 1979, Clay mineral assemblages as low grade metamorphic geothermometers: application to the thrust faulted disturbed belt of Montana, USA: Tulsa, Oklahoma, Society of Economic Paleontologists and Mineralogists, Special Publication, 26, 55-79.

Hower, J., Eslinger, E.V., Hower, M.E., Perry, E.A., 1976, Mechanism of burial metamorphism of argillaceous sediments: I. Mineralogical and chemical evidence: Geological Society of America Bulletin, 87, 727-737.

Hutcheon, I., Oldershaw, A., Ghent, E.D., 1980, Diagenesis of Cretaceous sandstones of the Kootenay Formation at Elk Valley (southeastern British Columbia) and Mt. Allan (southwestern Alberta): Geochimica et Cosmochimica Acta, 44, 1425-1435.

Inoue, A., Utada, M., 1991, Smectite-to-chlorite transformation in thermally metamorphosed volcanoclastic rocks in the Kamikita area, northern Honshu, Japan: American Mineralogist, 76, 628-640.

Jahren, J.S., Aagaard, P., 1992, Diagenetic illite-chlorite assemblages in arenites. I. Chemical evolution: Clays and Clay Minerals, 40, 540-546.

Jiang,, W.T., Peacor, D.R., 1994, Prograde transitions of corrensite and chlorite in low-grade pelitic rocks from the Gaspe Peninsula, Quebec: Clays and Clay Minerals, 42, 497-517.

Jiang, W.T., Peacor, D.R., Buseck, P.R., 1994, Chlorite geothermometry: contamination and apparent octahedral vacancies: Clays and Clay Minerals, 42, 593-605.

Karpova, G.V., 1969, Clay mineral post-sedimentary ranks in terrigenous rocks: Sedimentology, 13, 5-20.

Kopp, O.C., Fallis, S.M., 1974, Corrensite in the Wellington Formation, Lyons, Kansas: American Mineralogist, 59, 623-624.

Kubler, B., 1973, La corrensite, indicateour possible de milleux de sedimentation et du degree de transformation d'un sediment: Bulletin du Centre Recherche Pau-SNPA, 7, 543-556.

Laird, J., 1988, Chlorites: Metamorphic Petrology, *in* Bailey, S.W. (ed.), Hydrous phyllosilicates: Washington, D.C., Mineralogical Society of America, Reviews in Mineralogy, 19, 405-454.

López-Ramos, E., 1979, Geología de México: 2ª ed., México, Ed. Trillas, v. 3, p. 23-42.

Marsal, R.J., Mazari, M., 1962, El subsuelo de la Ciudad de México: México, Universidad Nacional Autónoma de México, Facultad de Ingeniería, 614 p.

Mering, J., Pedro, G., 1969, Discussion a propos des criteres de classification des phyllosilicates 2:1: Bulletin Groupe Francaise Argiles, 21, 1-30.

Meunier, A., Clement, J., Bouchet, A., Beaufort, D., 1988, Chlorite-calcite and corrensite-dolomite crystallization during two superimposed events of hydrothermal alteration in the "les Cetes" granite, Vosge, France: Canadian Mineralogist, 26, 413-422.

Mooser, F., 1956, Informe sobre la Geología de la Cuenca del Valle de México: México, Secretaría de Recursos Hidraúlicos, Comisión Hidrológica del Valle de México, 99 p.

Moore, D.M., Reynolds, R.C., 1997, X-ray diffraction and the identification and analysis of clay minerals: Oxford, Oxford University Press, 377 p.

Morse, S.A., 1980, Basalts and Phase Diagrams: New York, Springer-Verlag, 493 p.

Odin, G.S., 1985, La "verdine", facies granulaire vert, marin et cotier distinct de la glauconie: distribution actualle et composition: Comptes Rendus de l'Academie des Sciences de Paris, Serie II Mecanique, Physique, Chimie, Sciences de l' Universe, Sciences de la Terre, 301(2), 105-108.

Odin, G.S., Bailey, S.W., Amouric, M., Frohlich, F., Waychunas, G.S., 1988, Mineralogy of the verdine facies, *in* Odin, G.S. (ed.), Green marine clays; Oolitic ironstone facies, verdine facies, glaucony facies and celadonite-bearing facies, a comparative study: Amsterdam, Elsevier, Developments in Sedimentology, p. 159-206.

Pevear, D.R., Whitney, C.G., 1982, Clay minerals in Coast Range basalts of the Pacific Northwest: Eocene seafloor metamorphism, *in* Mumpton, Frederick A., (ed.), 19th Annual Meeting, Circum-Pacific Clay Minerals Society, Abstract volume: Hilo, Hawaii, Institute of Geophysics 6.

Reynolds, R.C. Jr., Reynolds, R.C.III., 1996, NEWMOD: the calculation of one dimensional x-ray diffraction patterns of mixed-layered clay minerals. Computer program: 8 Brook Road, Hanover, New Hampshire 03755, USA.

Rimmer, S.M., Eberl, D.D., 1982, Origin of an underclay as revealed by vertical variations in mineralogy and chemistry: Clays and Clay Minerals, 30, 422-430.

Roberson, H.E., 1989, Corrensite in hydrothermally altered oceanic rocks (abstract), *in* 26th Clay Minerals Society, Annual Meeting: Sacramento, The Clay Minerals Society, 59.

Roberts, B., Merriman, R.J., 1990, Cambrian and Ordovician metabentonites and relevance to the origin of associated mudrocks in the northern sector of the Lower Palaeozoic Welsh marginal basin: Geological Magazine, 127, 31-43.

Ruiz-Fernández, A., 1999, Distribución espacial y temporal de metales pesados en sedimentos lacustres de la Cuenca de México: Chalco, Texcoco y Cuauhtitlán Izcalli, estado de México: México, Universidad Nacional Autónoma de México, Unidad Académica de los Ciclos Profesionales y del Posgrado, Posgrado en Ciencias de la Tierra, Tesis doctoral, 101 p.

Schiffman, P., Staudigel, H., 1995, The smectite to chlorite transition in a fossil seamount hydrothermal system: the basement complex of La Palma, Canary Islands: Journal of Metamorphic Petrology, 13, 487-498.

Seyfried, W.E., Shanks, W.C., White, D.E., 1978, Clay mineral formation in DSDP leg 37 basalt: Earth and Planetary Science, 41, 265-276.

Shau, Y-H., Peacor, D., Essene, E., 1990, Corrensite and mixed-layer chlorite/corrensite in metabasalt from northern Taiwan: TEM/AEM, EPMA, XRD and optical studies: Contributions to Mineralogy and Petrology, 105, 123-142.

Sistema Hidraúlico del Distrito Federal, 1994, Cronología, *in* Departamento del Distrito Federal (ed.), Memoria de las obras del sistema de drenaje profundo del Distrito Federal: México, Departamento del Distrito Federal, I, 192 p.

Sudo, T., Takahashi, H., Matsui, H.,1954, Long spacing of 30 Å from a fire clay: Nature, 173, 161.

Sudo, T., Kodama, H., 1957, An aluminian mixed-layer mineral of montmorillonite-chlorite: Zeitschrift fur Kristallography, 109, 379-387.

Suquet, H., Pezerat, H., 1987, Parameters influencing layer stacking types in saponites and vermicullites: Clays and Clay Minerals, 35, 353-362.

Suquet, H., Pezerat, H., 1988, Comments on the classification of trioctahedral 2:1 phyllosilicates: Clays and Clay Minerals, 36, 184-186.

Suquet, H., Calle, C. de la, Pezerat, H., 1975, Swelling and structural organization of saponite: Clays and Clay Minerals, 23, 1-9.

Suquet, H., Iiyama, J.T., Kodama, H., Pezerat, H., 1977, Synthesis and swelling properties of saponites with increasing layer charge: Clays and Clay Minerals, 25, 231-242.

Urrutia-Fucugauchi, J., Lozano, S., Ortega, O., Caballero, M., Hansen, R., Bohnel, H., Negendank, J.F.W., 1994, Paleomagnetic and paleoenvironmental studies in the southern Basin of México. I. Volcanosedimentary sequence and basin structure of Chalco lake: Geofísica Internacional, 33, 421-430.

Vergo, N., April, R.H., 1982, Interstratified clay minerals in contact aureoles, West Rock, Connecticut: Clays and Clay Minerals, 30, 237-240.

Walker, J.R., Thompson, G.R., 1990, Structural variations in chlorite and illite in a diagenetic sequence from the Imperial Valley, California: Clays and Clay Minerals, 38, 315-321.

Weaver, C.E., 1989, Clays, muds and shales: Amsterdam, Elsevier, 819 p.

Willman, H.B., Glass, H.D., Frye, J.C., 1989, Glaciation and origin in the Geest in the Driftless Area of Northwestern Illinois: Illinois State Geological Survey, Circular, 535, 44.

Manuscript received: December 14 , 2000
Corrected manuscript received: November 30, 2001
Manuscript accepted: December 7, 2001